

Physics Results from RICH Detectors

Sheldon Stone¹

Syracuse University, Syracuse, NY 13244-1130

Abstract

RICH detectors have become extraordinarily useful. Results include measurement of solar neutrino rates, evidence for neutrino oscillations, measurement of TeV γ -rays from gravitational sources, properties of QCD, charm production and decay, and measurement of the CKM matrix elements V_{cs} , V_{cb} and V_{ub} . A new value $|V_{ub}/V_{cb}| = 0.087 \pm 0.012$ is determined.

.....

Invited talk at "The 3rd International Workshop on Ring Imaging Cherenkov Detectors," a research workshop of the Israel Science Foundation, Ein-Gedi, Dead-Sea, Israel, Nov. 15-20, 1998

¹ Supported by the National Science Foundation

1 Introduction

This paper describes some physics results obtained by experiments using Ring Imaging Cherenkov Detectors. Currently, the major physics issues are:

- What is the origin of mass? Another way of phrasing this question is to state that the Higgs boson must be found. This is a crucial reason for building the LHC machine. In this case, the RICH detectors have not yet been shown to have any relevance.
- Do neutrinos have mass? If so can neutrino mixing be explained in the context of the Standard Model?
- Does Quantum Chromo-Dynamics explain the strong interactions?
- How to unify gravity with the other interactions?
- Does the Standard Model explain quark mixing via the CKM matrix? We need to measure the CKM elements and CP violating angles.

The *raison d'etre* for RICH detectors is to answer these and other questions. The measurements reported here reflect my own view and may be incomplete.

RICH detectors can be viewed as being used for two distinct functions. One is to detect the presence of charged particles and the other is to identify the kinds of particles that have been detected by other devices.

2 QCD Results

One of the first RICH detectors was used in Fermilab experiment E605. They measured particle spectra produced in 800 GeV/c proton interactions with Be and W nuclei. The detector used a He gas radiator and a He-TEA photon detector. On average only 3 photo-electrons per track were detected. Yet results were produced [1].

More sophisticated modern versions of fixed target spectrometers are the CERN OMEGA spectrometer and SELEX at Fermilab [3]. A diagram of SELEX is shown in Fig. 1. Precision silicon strip detectors are interspersed with the target. A gas RICH detector with phototube readout is used to identify charged hadrons.

SELEX will study the decay of charmed baryons. They have already produced results on the production ratios of charmed mesons and baryons from different beams [4], shown in Fig. 2. These can be compared to theoretical models of charm production.

Two machines, LEP and SLC produce Z^0 bosons in e^+e^- collisions. Physics

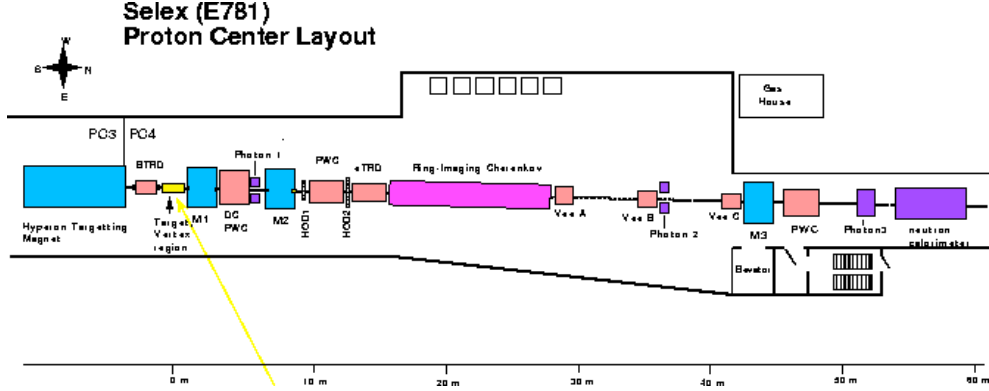


Fig. 1. Diagram of the Selex detector. The dashed arrow points to the vertex and target region, that contains the silicon strip modules.

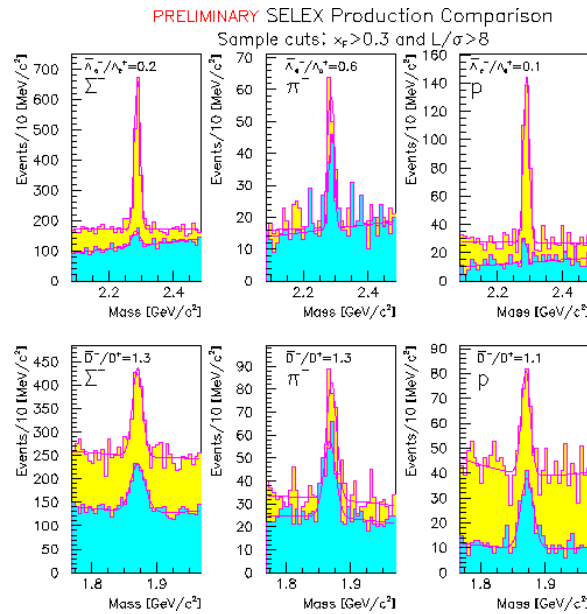


Fig. 2. Invariant mass plots for Λ_c^+ and D^+ and their antiparticles for different incidents beams. The measured production ratios are shown on the figure.

results have been obtained by two experiments using quite similar RICH detectors, DELPHI [5] at LEP and SLD [6] at SLC. A primitive sketch of the RICH systems is shown in Fig. 3. These systems use both liquid C_6F_{14} and gaseous fluorine radiators. The Cherenkov photons are converted in TMAE and drifted using a TPC to proportional wires. The performance of the SLD CRID has been characterized in terms of efficiency and rejection for a particular set of analysis criterion. Shown in Fig. 4(left) are efficiencies for the wanted hadron and the efficiency for the unwanted species (really rejection).²

The Z^0 decays into quark-antiquark pairs or lepton-antilepton pairs. In the case of the quarks, the energy ends up in hadrons and the momentum spectrum

² In general, the efficiency versus rejection is a function of the analysis cuts and can be chosen differently to optimize each study.

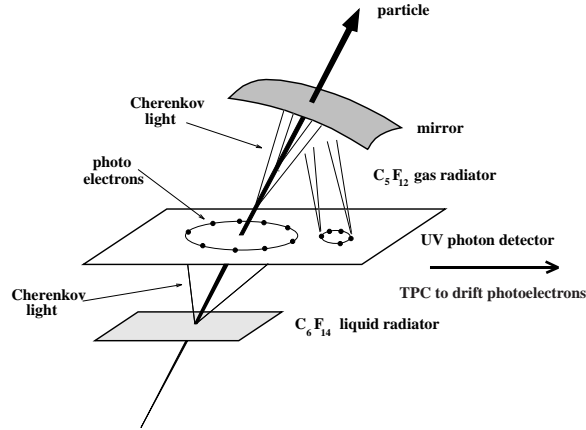


Fig. 3. A sketch of the DELPHI RICH and SLD CRID systems.

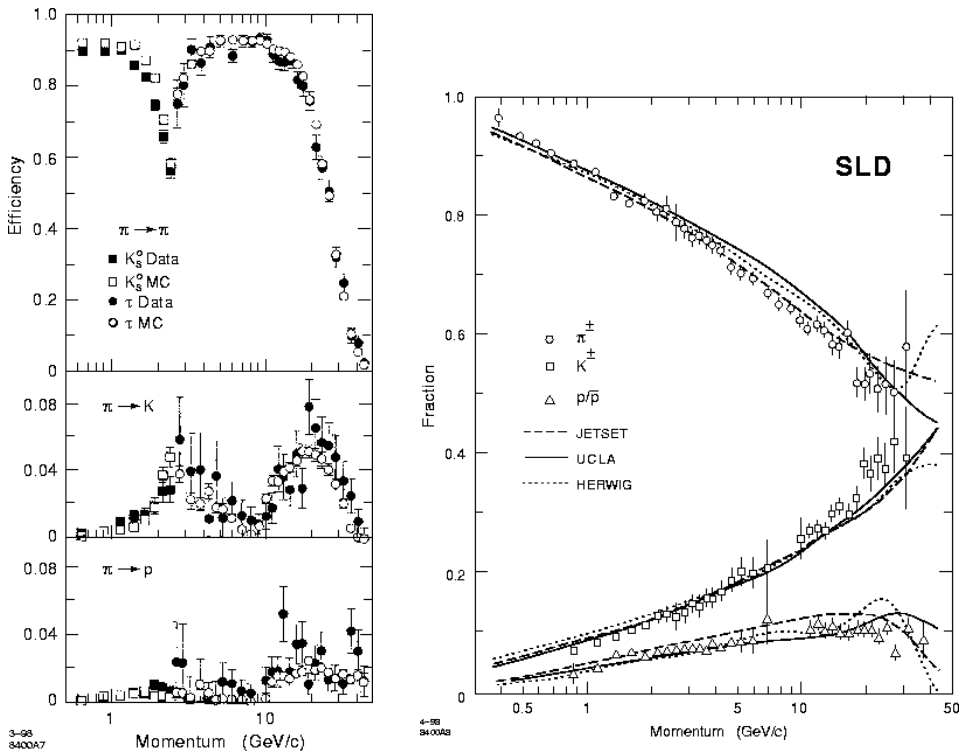


Fig. 4. (Left) Efficiencies for tracks from K_s^0 (squares) and τ^\pm (circles) decays to be identified as each hadron species in the SLAC CRID. The solid symbols show the data and the open symbols the simulation. (Right) Comparison of measured charged hadron fractions (symbols) from SLD compared with the predictions of various fragmentation models.

of the hadron species can be compared with models of this fragmentation. The particle spectrum from Z^0 decays has been measured by both DELPHI and SLD. The SLD spectrum is shown in Fig. 4(right) and compares well with the different models [7].

QCD predicts the presence of a new state of matter, a so called “quark-gluon plasma,” that may be produced in the collisions of heavy nuclei. Evidence

could come dileptons produced in elementary collisions such as $q\bar{q} \rightarrow \ell^+\ell^-$. Electron pairs are typically searched for. They can also come from more mundane sources, such as vector meson decays or Dalitz decays.

The CERES experiment has searched for e^+e^- pairs in heavy ion collisions at the CERN SPS. A sketch of the detector is shown in Fig. 5(left). They have two RICH detectors using a CH_4 gas radiator and UV (TMAE based) photon detectors, which are placed outside the region of the collision products [8]. Also, heavier particles, such as pions, tend not to radiate, so this type of system is sometimes called “hadron blind.”

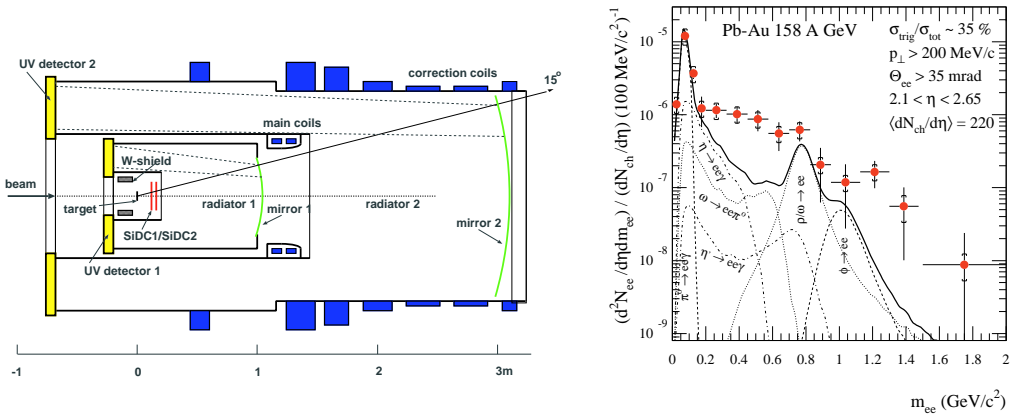


Fig. 5. (Left) Sketch of the CERES detector. (Right) The cross-section for e^+e^- pairs as a function of dilepton mass. The yield from expected sources is also shown. The statistical errors (bars) and the systematic errors (brackets) are plotted independently of each other.

Fig. 5(right) shows the results for Pb-Au collisions [9]. There is an excess of e^+e^- pairs above the estimated background sources. Many new experiments are being built to explore this phenomena including HADES at GSI Darmstadt, and RHIC experiments at Brookhaven.

3 Water Cherenkov Detectors

3.1 Introduction

The quest for a theory to unify strong and electroweak interactions led to models based on higher symmetry groups which predicted or at least allowed the possibility of proton decay. The IMB and Kamiokande detectors were large tanks of pure water placed deep underground to minimize the cosmic ray background. The water provided the protons that might decay and also the

means of detection using the Cherenkov light produced by the decay products. Kamiokande was greatly enlarged to Super-Kamiokande [12].

All these detectors have many large diameter photomultiplier tubes which gather the unfocused light (proximity focused in Tom Ypsilantis terminology). They can detect charged leptons and hadrons and also photons that convert to pairs in the water. They can discriminate between electrons and muons because the electrons scatter more. Fig 6 shows the phototubes hit by an electron and muon. The width of the Cherenkov ring is much smaller in the muon case.

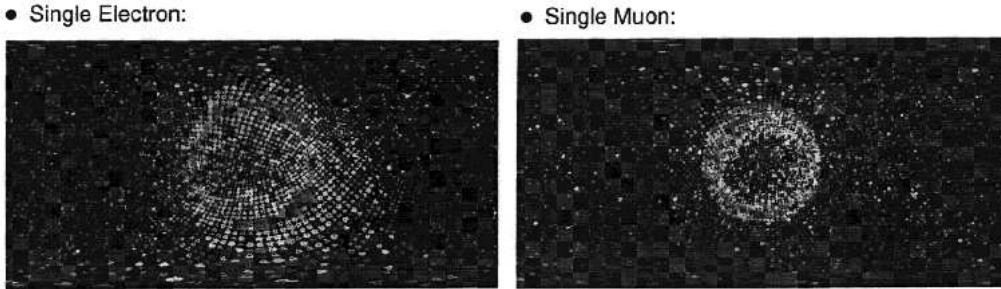


Fig. 6. Examples of the detector response of an electron and a muon in Super-Kamiokande.

These detectors can also detect ν_e from the sun and from supernovas. The latter capability was impressively demonstrated by detecting the explosion of supernova 1987A [13]. They also can detect neutrinos produced in the atmosphere from cosmic ray interactions.

3.2 The Atmospheric Neutrino Anomaly

Cosmic rays, mostly protons, hit the atmosphere and interact at altitudes of ten to twenty kilometers above the Earth's surface. Naively, we expect two muon-neutrinos, ν_μ , for every ν_e , because of the dominant decay chains $\pi^+(K^+) \rightarrow \mu^+\nu_\mu$; $\mu^+ \rightarrow e^+\nu_e\bar{\nu}_\mu$ (and similarly for $\pi^-(K^-)$). IMB first observed that the ratio was about half of what was expected [14]. The data from several experiments are shown in Fig. 7.

Although some experiments did not see the anomaly, the precise data from Kamiokande and Super-Kamiokande [16] clearly show that IMB was correct. The question remained, however, was there something wrong in the expectation or was the effect coming from a loss of ν_μ due to neutrino oscillations?

In neutrino oscillations, different species can metamorphose into other ones. We have three known species of neutrinos, ν_e , ν_μ and ν_τ . If ν 's have mass

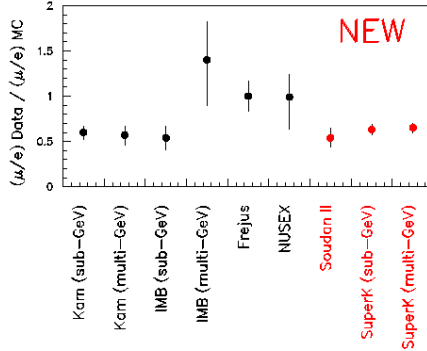


Fig. 7. Summary of measurements of the atmospheric neutrino ratio of measured muon/electron neutrino rates divided by the expectation as given by Monte Carlo prediction. $(\nu_\mu/\nu_e)_{data}/(\nu_\mu/\nu_e)_{MC}$ for atmospheric experiments. The three newest results are listed at the right (from ref. [15]).

they can transform from one to another. Specifically, the probability that a neutrino, ν_i , not oscillate is given by

$$P(\nu_i \rightarrow \nu_i) = 1 - \sin^2(2\theta) \sin^2\left(1.27\Delta m^2 \frac{L}{E_\nu}\right), \quad (1)$$

where θ is the unknown mixing angle, Δm is the unknown mass difference, L is the distance from the production point and E_ν the energy.

Cosmic rays hitting the upper atmosphere are distributed uniformly. The experiment is at a fixed point close to the Earth's surface. If a neutrino comes from directly overhead the cosine of its angle is defined as +1, while those coming through the earth have a cosine of -1. Thus ν 's have different path lengths to get to the detector; since the ν energy spectrum is the same from any direction, we can vary the ratio L/E_ν by looking at different angles. These ν 's range from below 1 GeV to many GeV in energy. (Super-Kamiokande defines sub-GeV to be <1.3 GeV, and multi-GeV to be larger.)

Super-Kamiokande is a large enough detector to get enough atmospheric neutrino events to be able to show angular distributions. While ν_e behave as expected, the distribution of ν_μ do not. In Fig. 8(left) the zenith angle distribution of ν_μ is shown along with the expectations based on simulation. There is a clear deficit of up-going neutrinos. On the right side the L/E_ν distribution is plotted for both ν_e and ν_μ . The evidence for ν_μ oscillating into something is clear for ν_μ . The dashed lines show the expected shape for $\nu_\mu \Leftrightarrow \nu_\tau$ using $\Delta m^2 = 2.2 \times 10^{-3} eV^2$ and $\sin^2(2\theta)=1$. The dashed lines for ν_e show the expected shape without oscillations. The slight L/E_ν dependence for e -like events is due to contamination (2-7%) of ν_μ .

If the ν_μ are oscillating, they can change into ν_e , ν_τ or some other species of

yet unobserved neutrino. As the latter possibility is less likely, let us ignore it here. We do not see an increase in ν_e , so its most likely that the ν_μ are changing into ν_τ . Unfortunately, the ν_τ are not energetic enough to produce τ^- via a charged current interaction, most of the time.

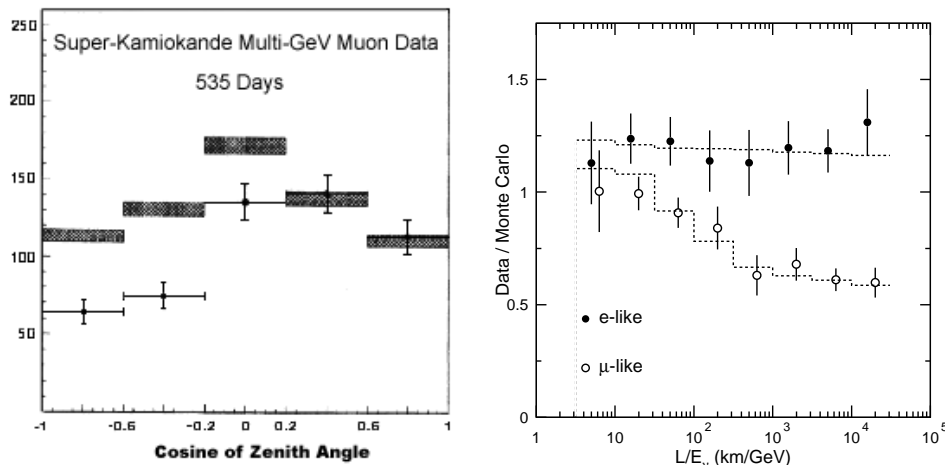


Fig. 8. (Left) Zenith angle distributions of ν_μ multi-GeV events. Upward-going particles have $\cos\theta < 0$ and downward-going particles have $\cos\theta > 0$. The shaded region shows the Monte Carlo expectation for no oscillations normalized to the data live-time with statistical errors. (Right) The ratio of data to Monte Carlo versus reconstructed L/E_ν (fully contained events only) [16].

3.3 The Solar Neutrino Anomaly

Thermonuclear reactions in the center of the sun are a prolific source of ν_e . Detecting them and comparing the rate with models describing the process have gone on since 1964, starting with Ray Davis' pioneering experiment in the Homestake mine [17]. Confirmation that the rate is about half what is expected was made by the Gallium based experiments (Gallex and Sage) [18] and the water Cherenkov detectors [19]. The expected flux, and the results are shown in Fig. 9.

Super-Kamiokande can also show that the detected ν_e come from the sun. Fig 10 shows the angle of the produced electron with respect to the solar direction [19]. The sharp peak is evident above the flat background.

One explanation of the ν_e deficit is that the sun is just at the right distance from the earth that half have oscillated to other species. This is called the “Just So,” solution [20]. Another explanation is there is a resonant enhancement of oscillations due to the high electron density in the sun's core; this is called the MSW effect [21].

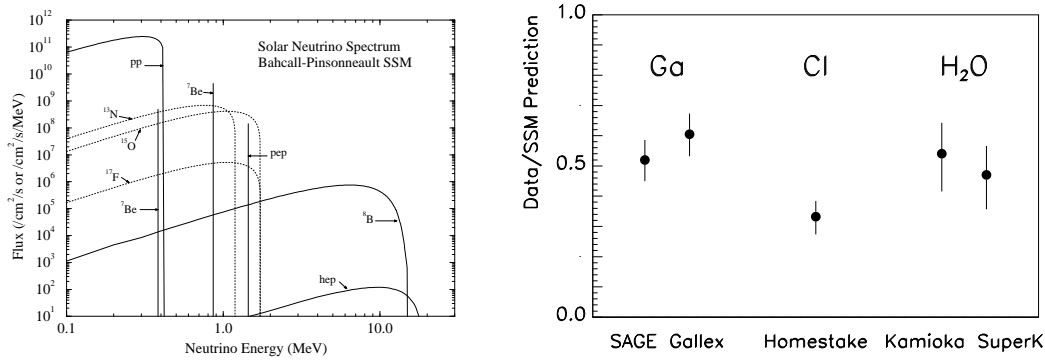


Fig. 9. (Left) The predicted solar neutrino energy spectrum. The nuclear reactions are indicated. (Right) The measured solar neutrino flux from the different experiments divided by the expectations of the standard solar flux model. Gallium experiments are sensitive above 0.23 MeV, Cl above 0.8 MeV, and H₂O above 6.5 MeV, from [15].

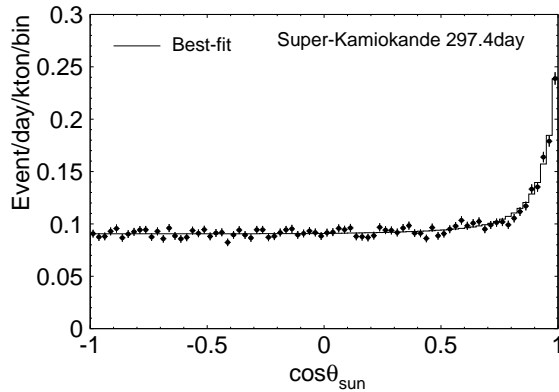


Fig. 10. The solar neutrino spectrum from Super-Kamiokande as a function of the angle with respect to the sun.

3.4 Summary of Neutrino Oscillation Signals and Future Prospects

Possible signals for neutrino oscillations come from three sources, two of which, atmospheric neutrinos and solar neutrinos have been described here. A third source, the LSND experiment claims observation of a signal for $\bar{\nu}_\mu \rightarrow \bar{\nu}_e$ [22]. Putting these on the same $\Delta m^2 - \sin^2(2\theta)$ plot (Fig. 11) shows that it will be difficult to reconcile all three measurements.

In the near term future there will be several new experiments using Water Cherenkov detectors that should reveal much about the mysteries just beginning to be revealed. A beam of ν_μ will be directed at Super-Kamiokande [23]. The SNO detector, a large D₂O detector will be able to detect the neutral current neutrino interactions and thus be able to measure the total atmospheric neutrino flux and the total solar flux as well as charged current interactions

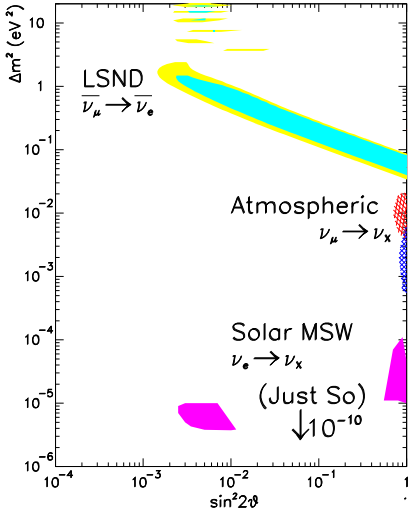


Fig. 11. Allowed regions for three indications of neutrino oscillations. The top blob for Atmospheric is from Kamiokande while the bottom is for Super-Kamiokande (from ref. [15]).

[24]. Borexino will start and be able to detect 0.86 MeV neutrinos from solar Be^7 reactions at the level of 50 events/day [25].

4 Measurement of Primary Cosmic Rays with Caprice

Analysis of the atmospheric neutrino data relies on knowledge of the primary cosmic ray flux. The Caprice experiment has taken data with a magnetic spectrometer incorporating a RICH detector with a NaF radiator and photon detector using a wire-proportional chamber filled with TMAE and ethane [26]. They also have tracking and an electromagnetic calorimeter.

CAPRICE has measured the rates of many species at the top of the atmosphere. The response to positive tracks is shown in Fig. 12(left). Their primary cosmic ray (mostly proton) flux measurement [27] is compared with others in Fig. 12(right). The data that shows a larger rate is from older measurements. They have also measured the \bar{p}/p rate to be $\sim 10^{-4}$, $\mu^+/\mu^- = 1.64 \pm 0.08$ and e^+/e^- to be ~ 0.1

Calculations of the primary cosmic ray flux and their interactions with air, producing secondary mesons that then decay into leptons and neutrinos are important in evaluating the total neutrino yield and less consequential in evaluating the angular distribution of the ν_μ/ν_e ratio. Super-Kamiokande uses several calculations of primary cosmic ray flux [29][30]. The HKKM [29] calculation of the primary cosmic ray flux is shown as “Mid” on Fig. 12(right). Francke has argued at this meeting that the HKKM calculation over estimates

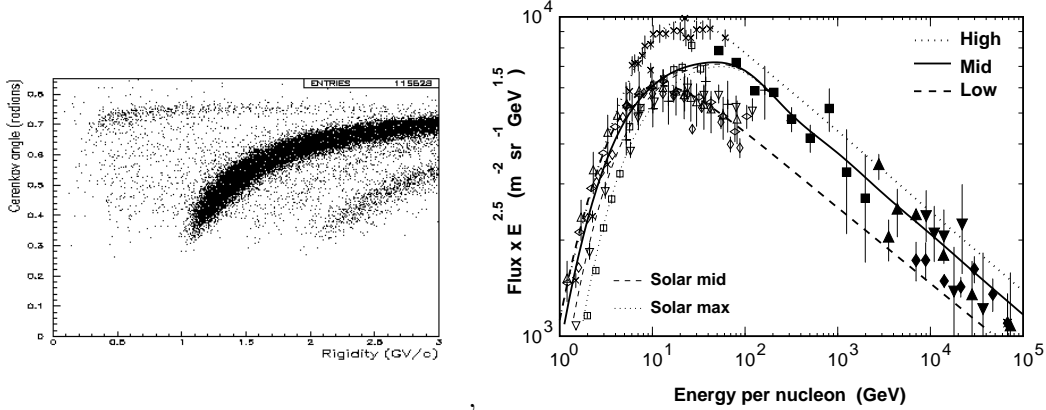


Fig. 12. (Left) Cherenkov angle as a function of rigidity, R , for positive particles in CAPRICE, where $R = (A/Q)(E^2 + 2M_oE)^{1/2}$, $M_o=0.9315$ GeV, A is atomic mass number, and Q is charge. The bands, top to bottom, correspond to μ^+ , p and He nuclei. (Right) Measured primary cosmic ray proton flux. The CAPRICE data are shown by open vertical diamonds [27]. Other data are described in ref. [28]. The labels High, Mid and Low refer to the ranges of fluxes used by HKKM [28].

the CAPRICE data by about a factor of two. This could lead to some reinterpretation of the atmospheric neutrino data and may change the limits in the $\Delta m^2 - \sin^2(2\theta)$ plane.

5 Gravitational Physics with Cherenkov Detectors

The Fly's Eye detector in Utah uses scintillation light to detect ultra-relativistic cosmic rays [31]. Cherenkov light produced in the atmosphere from TeV γ -rays, after converting to e^+e^- pairs can also be used. HEGRA incorporates several Cherenkov light detectors with scintillation detection of electromagnetic particles, and muon detection over an area of 200x200 m² [32].³

One example of what they have observed is shown in Fig. 13. They measured a high flux of TeV γ rays from the source Mkn501. The energy spectrum follows a power law from 1-10 TeV. Furthermore, the source intensity varies from half that of the Crab Nebula to six times in very small time intervals. This phenomena has not been explained, but clearly these measurements will lead to an increased understanding of gravitational physics phenomenology [33].

6 Measurement Of The Cabibbo-Kobayshi-Maskawa Matrix

³ For a description of other Cherenkov air shower experiments, see E. Lorentz in these proceedings.

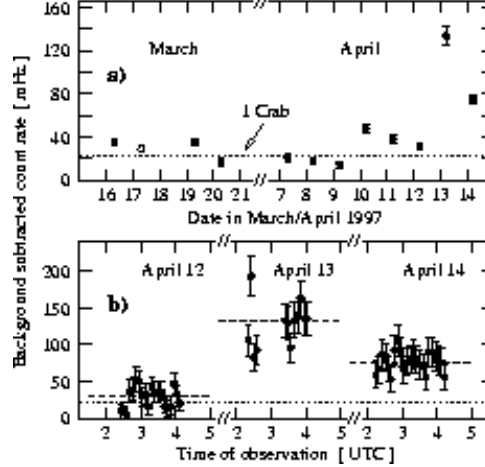


Fig. 13. Detection rate of Mkn 501 on a night by night basis (a) for the whole data set and in 5 min. intervals (b) for the last 3 nights. The dashed lines give the average per night, the dotted line gives the Crab rate.

6.1 Introduction

In the “Standard Model” of Electroweak interactions, the gauge bosons, W^\pm , γ and Z^0 couple to mixtures of the physical d , s and b quark states. This mixing is described by the Cabibbo-Kobayashi-Maskawa (CKM) matrix [34].

$$V_{CKM} = \begin{pmatrix} V_{ud} & V_{us} & V_{ub} \\ V_{cd} & V_{cs} & V_{cb} \\ V_{td} & V_{ts} & V_{tb} \end{pmatrix}, \quad (2)$$

where the subscripts refer to the quarks. In the Wolfenstein approximation⁴ the matrix is written in terms of the parameters λ , A , ρ and η as [35]

$$V_{CKM} = \begin{pmatrix} 1 - \lambda^2/2 & \lambda & A\lambda^3(\rho - i\eta) \\ -\lambda & 1 - \lambda^2/2 & A\lambda^2 \\ A\lambda^3(1 - \rho - i\eta) & -A\lambda^2 & 1 \end{pmatrix} \quad (3)$$

These parameters are **fundamental constants** of nature that need to be determined experimentally, as is required for other fundamental constant such as α or G .

⁴ In higher order other terms have an imaginary part; in particular the V_{cd} term becomes $-\lambda - A^2\lambda^5(\rho + i\eta)$, which is important for CP violation in K_L^0 decay.

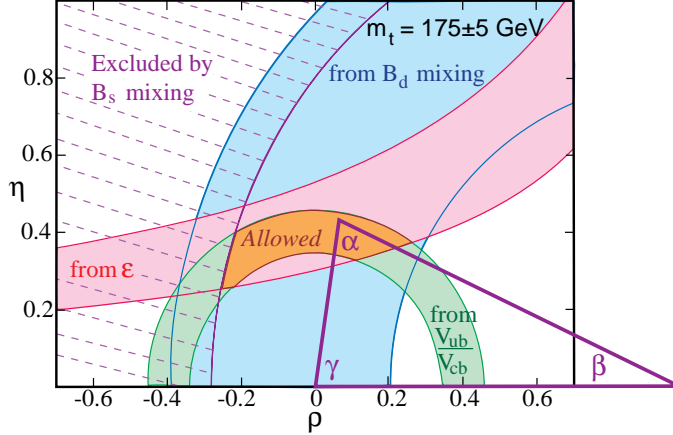


Fig. 14. The regions in $\rho - \eta$ space (shaded) consistent with measurements of CP violation in K_L^0 decay (ϵ), V_{ub}/V_{cb} in semileptonic B decay, B_d^0 mixing, and the excluded region from limits on B_s^0 mixing. The allowed region is defined by the overlap of the 3 permitted areas, and is where the apex of the CKM triangle sits. The bands represent $\pm 1\sigma$ errors. The error on the B_d mixing band is dominated by the parameter f_B . Here the range is taken as $240 > f_B > 160$ MeV. $|V_{ub}/V_{cb}|$ is taken as 0.087 ± 0.012 (see section 6.3).

The constants λ and A are determined from charged-current weak decays, and are 0.22 and ~ 0.8 , respectively [36]. The η term gives rise to a complex phase in the matrix which allows CP violation in weak interactions. A similar matrix may exist for ν 's, if they have mass. It would explain ν mixing and predict the possibility of CP violation in ν interactions.

Although ρ and η have not been determined, there are measurements that provide constraints on their value. These include CP violation in K_L^0 decay, characterized by the value ϵ , $B^0 \leftrightarrow \bar{B}^0$ mixing and V_{ub}/V_{cb} . My interpretation of the current status of these measurements is shown in Fig. 14. Here I have used only $\pm 1\sigma$ errors, with the caveat that the dominant errors in all three cases are caused by estimates of uncertainties on theoretical parameters.

Study of these processes has suffered from lack of particle identification capabilities. CLEO and ARGUS had time-of-flight scintillators and dE/dx measurements from the tracking chamber [37]. However, they are blind to K/π separation between $\sim 1 - 2.2$ GeV/c with poor separation above 2.2 GeV/c. Yet CLEO was the first to measure $|V_{ub}/V_{cb}|$ and both made the first relatively precise measurements of $|V_{cb}|$. Recently, the DELPHI RICH has brought some improvements, which point to future possibilities.

6.2 Measurement Of V_{cb} Using $B \rightarrow D^* \ell \nu$

Currently, the most favored technique is to measure the decay rate of $B \rightarrow D^* \ell^- \bar{\nu}$ at the kinematic point where the D^{*+} is at rest in the B rest frame (this is often referred to as maximum q^2 or $\omega = 1$). Here, the theoretical uncertainties are at a minimum.⁵ There have been previous results using this technique using the decay sequence $D^{*+} \rightarrow \pi^+ D^0$; $D^0 \rightarrow K^- \pi^+$, or similar decays of the D^{*0} .

In a recent analysis, DELPHI detects only the slow π^+ from the D^{*+} decay and does not explicitly reconstruct the D^0 decay [39]. The RICH helps in measuring missing energy in this complicated measurement. The distribution of events with respect to ω is shown in Fig. 15. The dip in the data near ω of one is an artifact caused by the drop in efficiency in detecting the slow π^+ at low momentum. Still, the decay rate can be ascertained. Table 1 summaries determinations of V_{cb} . Here, the first error on is statistical, the second systematic and the third, an estimate of the theoretical accuracy in predicting the form-factor at ω of 1. Currently, DELPHI has the smallest error, however, CLEO has only used 1/6 of their current data and will certainly improve on this measurement. The quoted average $|V_{cb}| = 0.0381 \pm 0.0021$ combines the averaged statistical and systematic errors with the theoretical error in quadrature and takes into account the common systematic errors, such as the D^* branching ratios.

Table 1

Modern Determinations of V_{cb} using $B \rightarrow D^* \ell^- \bar{\nu}$ decays at $\omega = 1$

Experiment	$V_{cb} (\times 10^{-3})$
DELPHI [39]	$41.2 \pm 1.5 \pm 1.8 \pm 1.4$
ALEPH [40]	$34.4 \pm 1.6 \pm 2.3 \pm 1.4$
OPAL [41]	$36.0 \pm 2.1 \pm 2.1 \pm 1.2$
CLEO [42]	$39.4 \pm 2.1 \pm 2.0 \pm 1.4$
Average	38.1 ± 2.1

6.3 Measurement Of V_{ub}

Another important CKM element that can be measured using semileptonic decays is V_{ub} . The first measurement of V_{ub} done by CLEO and subsequently confirmed by ARGUS, used only leptons which were more energetic than those

⁵ Current estimates of the form-factor necessary to translate the decay rate measurement into a value are 0.91 ± 0.03 [38].

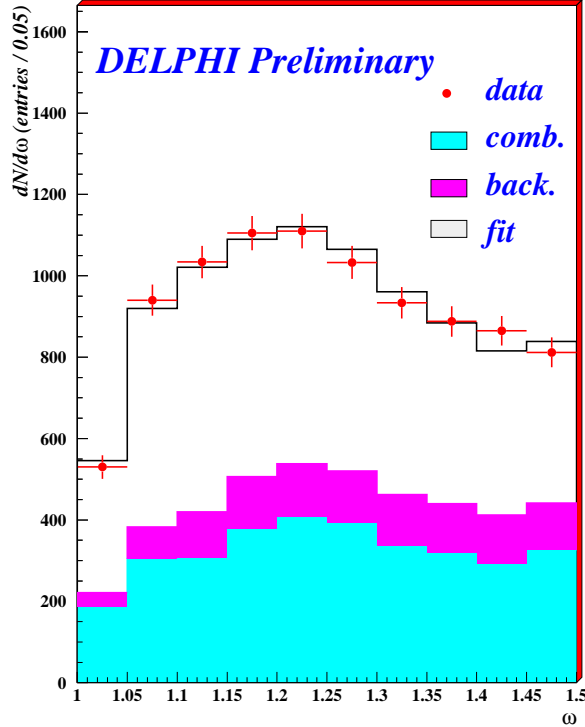


Fig. 15. Fit to the ω distribution from DELPHI. The solid points are the data, the light shaded area corresponds to combinatorial background, the dark shaded area correspond to other background and the horizontal line contains these components plus the signal.

that could come from $b \rightarrow c\ell^{-}\bar{\nu}$ decays [43]. These “endpoint leptons” can occur, $b \rightarrow c$ background free, at the $\Upsilon(4S)$ because the B ’s are almost at rest. Unfortunately, there is only a small fraction of the $b \rightarrow u\ell^{-}\bar{\nu}$ lepton spectrum that can be seen this way, leading to model dependent errors in extracting final values.

DELPHI tries to isolate a class of events where the hadron system associated with the lepton is enriched in $b \rightarrow u$ and thus depleted in $b \rightarrow c$ [44]. They define a likelihood that hadron tracks come from b decay by using a large number of variables including, vertex information, transverse momentum, not being a kaon. Then they require the hadronic mass to be less than 1.6 GeV, which greatly reduces $b \rightarrow c$, since a completely reconstructed $b \rightarrow c$ decay has a mass greater than that of the D (1.83 GeV). They then examine the lepton energy distribution for this set of events, shown in Fig. 16.

DELPHI finds $|V_{ub}/V_{cb}| = 0.104 \pm 0.12 \pm 0.015 \pm 0.009$. The first error is statistical, the second systematic and the third the uncertainty quoted by Uraltsev on his model that allows the extraction of $|V_{ub}|$ from the measured branching ratio [45]. The systematic error is larger than the statistical error. This reflects the extensive modeling of the $b \rightarrow c$ decays. The theoretical error is estimated at 8%. However, another calculation using the same type of model

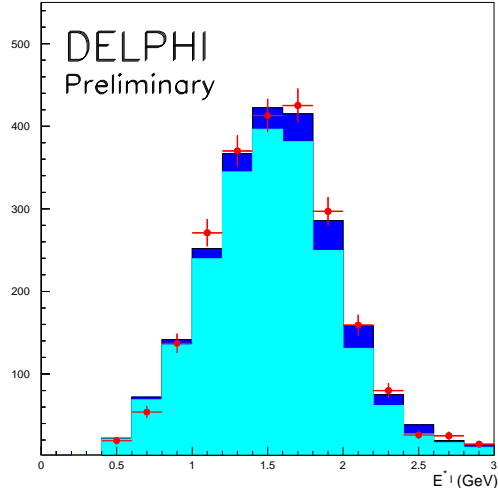


Fig. 16. The lepton energy distribution in the B rest frame from DELPHI. The data have been enriched in $b \rightarrow u$ events, and the mass of the recoiling hadronic system is required to be below 1.6 GeV. The points indicate data, the light shaded region, the fitted background and the dark shaded region, the fitted $b \rightarrow u\ell\nu$ signal. The theoretical models are described in ref. [47].

by Jin [46] gives a 14% lower value, with a quoted error of 10%.

ALEPH [48] and L3 [49] have used techniques similar to DELPHI. I have averaged all three LEP results and shown them in Fig. 17 without any theoretical error. My best estimate of $|V_{ub}/V_{cb}|$ using this technique includes a 14% theoretical error added in quadrature with a common systematic error of 14%, since the Monte Carlo calculations at LEP are known to be strongly correlated.

Also shown in Fig. 17 are results from CLEO using the measured the decay rates for the exclusive final states $\pi\ell\nu$ and $\rho\ell\nu$ [51], and results from endpoint leptons, dominated by CLEO II [50]. From the exclusive results, the model of Korner and Schuler (KS) is ruled out by the measured ratio of ρ/π . This model deviated the most from the others used to get values of $|V_{ub}|$ from endpoint leptons. Thus the main use of the exclusive final states has been to restrict the models. The endpoint lepton results are statistically the most precise. Assigning a model dependent error is quite difficult. I somewhat arbitrarily have assigned a 14% irreducible systematic error to these models and used the average among them to derive a value. My best overall estimate is that $|V_{ub}/V_{cb}| = 0.087 \pm 0.012$.

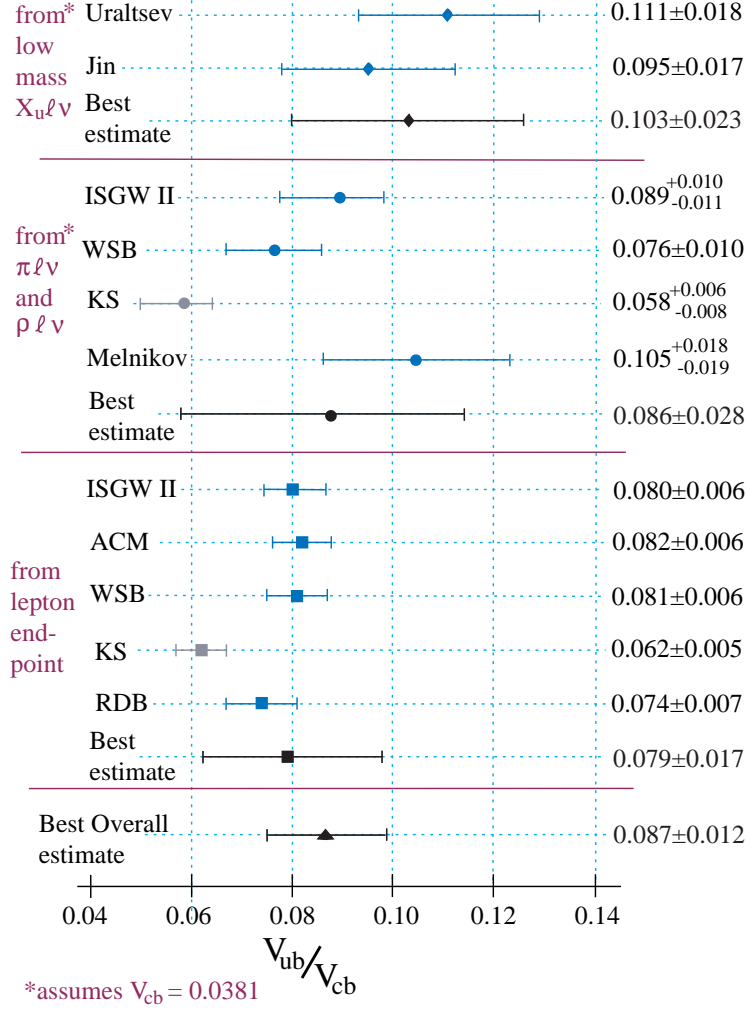


Fig. 17. Measurements of $|V_{ub}/V_{cb}|$ using different techniques and theoretical models [47]. (The KS model has been ruled out.)

6.4 Measurement of V_{cs}

Using the reaction $e^+e^- \rightarrow W^+W^-$ at LEP II DELPHI has directly measured the CKM element V_{cs} . There are two ways that LEP II experiments have estimated this value. One way, is to measure the branching ratio of the W 's into hadrons and use the sum rule:

$$|V_{cs}| = \sqrt{\frac{3\Gamma_\ell}{\Gamma_h} \frac{Br(W^\pm \rightarrow hadrons)}{(1 - Br(W^\pm \rightarrow hadrons))} - \sum_{ij \neq cs} |V_{ij}|^2}, \quad (4)$$

where Γ_ℓ and Γ_h , are the leptonic and hadronic widths of the W^\pm .

A better way, which does not rely on other measurements to measure the ratio directly of $Br(W \rightarrow \bar{c}s)/Br(W \rightarrow \text{hadrons})$. For this DELPHI uses the RICH to identify kaons, which come not only from the s quark but are also prolifically produced in \bar{c} decays. Using this method DELPHI finds

$$|V_{cs}| = 1.01_{-0.10}^{+0.12} \pm 0.10, \quad (5)$$

which is by far the best direct measurement of this quantity, and is consistent with the expected value of 0.95. This is important because it checks the predictions of the CKM hypothesis.⁶

7 Conclusions

It takes a Village to build a RICH, a village of knowledge cultivated at this conference. There are several different technologies: gas, H₂O, and crystal radiators coupled with gas, CsI, phototube photo-electron detectors, producing great results in neutrino physics, b decays and QCD. We expect even more interesting results soon!

8 Acknowledgments

I thank Amos Breskin and Rachel Chechik for arranging an excellent meeting. My colleagues Marina Artuso, Ray Mountain and Tomasz Skwarnicki helped on various aspects of this talk.

⁶ The indirect method gives $|V_{cs}| = 0.98 \pm 0.07 \pm 0.04$.

References

- [1] R. L. McCarthy et al., *Nucl. Instr. and Meth. A* **248** (1986) 69; P. B. Straub et al., *Phys. Rev. Lett.* **68** (1992) 452.
- [2] U. Müller et al., *Nucl. Instr. Meth. A* **371** (1996) 27.
- [3] M. Procario, *Physics Goals and Status of SELEX: Fermilab E781*. Talk at Conference on Intersections of Particle and Nuclear Physics, Montana, June 1997; J. Engelfried et al. *The SELEX Phototube RICH Detector*, FERMILAB-Pub-98/299-E, hep-ex/9811001.
- [4] A. Kushnirenko, *Charm physics results from SELEX*, Talk on Heavy Quarks at fixed target HQ98 conference. Fermilab, October 1998, to appear in proceedings.
- [5] W. Adam et al. (DELPHI), *Nucl. Instr. and Meth. A* **367** (1995) 233.
- [6] K. Abe et al. (SLD), *Nucl. Instr. and Meth. A* **343** (1994) 74.
- [7] A. C. Benvenuti et al., *Production of π^+ , K^+ , K^0 , B , K^{*0} , ϕ , p and Λ^0 In Hadronic $C. Z^0$ Decays*, SLAC-PUB-7766 (1998).
- [8] G. Agakieiev et al. (CERES), *Nucl. Instr. Meth. A* **371** (1996) 16.
- [9] G. Agakieiev et al. (CERES), *Nucl. Phys. A* **638** (1998) 159c.
- [10] R. Becker-Szendy et al. (IMB), *Nucl. Instr. and Meth. A* **324** 1993 (363).
- [11] M. Nakahata et al. (Kamiokande), *J. Phys. Soc. Jpn.* **55** (1986) 2786.
- [12] K. Inoue, in TAUP97, *5th Int. Workshop on topics in Astroparticle and Underground Physics*, Sept. 1997, Laboratori Nazionali del Gran Sasso, Italy.
- [13] R. M. Bionta et al. (IMB), *Phys. Rev. Lett.* **58** (1987) 1494; K. Hirata et al. (Kamiokande) *Phys. Rev. Lett.* **58** (1987) 1490.
- [14] J.M. LoSecco et al. (IMB), *Phys. Rev. Lett.* **54** (1985) 2299; D. Casper et al. (IMB-3) *Phys. Rev. Lett.* **66** (1991) 2561.
- [15] J. M. Conrad, *Recent Results on Neutrino Oscillations*, presented at the XXIX Int. Conf. on High Energy Physics, Vancouver, hep-ex/9811009 (1998), to be published in proceedings; and references contained therein.
- [16] Y. Fukuda et al. (Super-Kamiokande), *Phys. Rev. Lett.* **81** (1998) 1562.
- [17] R. Davis, *Prog. Part. Nucl. Phys.* **32**, (1994) 13.
- [18] J. N. Abdurashitov et al., *Phys. Lett. B* **328** (1994) 234; P. Anselmanni et al., *Phys. Lett. B* **328** (1994) 377.
- [19] Y. Fukuda et al. (Super-Kamiokande), *Phys. Rev. Lett.* **81** (1998) 1158; Erratum- *ibid.* **81** (1998) 4279; M. Vagins, *SuperK Solar Neutrinos*, presented at XXIX Int. Conf. on High Energy Physics, Vancouver, 1998, to be published in proceedings.

- [20] V. N. Gribov and B. M. Pontocorvo, *Phys. Lett B* **28** (1969)493.
- [21] L. Wolfenstein, *Phys. Rev. D* **17** (1978) 2369; S. P. Mikheyev and A. Yu. Smirnov, *Yad. Fiz* **42** (1985) 1441 [*Sov. J. Nucl Phys.* **42** (1985) 913]; *Nuovo Cimento C* **9** (1986) 17.
- [22] C. Athanassopoulos et al.(LSND), *Phys. Rev. Lett.* **81** (1998) 1774.
- [23] Y. Oyama, *K2K (KEK to Kamioka) neutrino-oscillation experiment at KEK-PS*, presented at the YITP workshop on flavor physics, Kyoto (1998) hep-ex/9803014.
- [24] B. C. Robertson, *SNO: A Multifunction Spectrometer For Solar Neutrinos*, In *Villars sur Ollon 1993, Perspectives in neutrinos, atomic physics and gravitation* 119; See also <http://www.sno.phy.queensu.ca/~> .
- [25] G. Ranucci et al. (Borexino), *Nucl. Phys. Proc. Suppl.* **70** (1999) 377.
- [26] G. Barbiellini et al. (Caprice), *Nucl. Instr. and Meth.* A371 (1996) 169.
- [27] T. Francke, in these proceedings; G. Barbiellini et al. (Caprice), *A Measurement of the Proton Spectrum at 1 AU Near Solar Minimum with the Caprice Experiment*, In *Proc. 25th International Cosmic Ray Conference, Durban*, (1997) 369.
- [28] See references for data used in Fig. 1. in M. Honda, *Uncertainty of the atmospheric neutrino fluxes*, presented at Neutrino98, Takayama, Japan, June, (1998), hep-ph/9811504.
- [29] M. Honda et al., *Phys. Rev. D* **52** (1995) 4985.
- [30] T. K. Gaisser et al., *Phys. Rev. D* **54** (1996) 5578; G. Barr et al., *Phys. Rev. D* **39** (1989) 3552; V. Agrawal et al., *Phys. Rev. D* **53** (1996) 1314; T. K. Gaisser and T. Stanev, in *Proc. 24th Int. Cosmic Ray Conf., Rome, Vol 1* (1995) 694.
- [31] See <http://nevis1.nevis.columbia.edu/~hires/hires.html>
- [32] F.A. Aharonian, G. Heinzlmann, *Nucl. Phys. Proc. Suppl.* **60B** (1998) 193.
- [33] F. Aharonian et al. (HEGRA), *The Temporal Characteristics of the TeV Gamma-Radiation from Mkn 501 in 1997, I: Data from the Stereoscopic Imaging Atmospheric Cherenkov Telescope System of HEGRA*, (1998) astro-ph/9808296.
- [34] N. Cabibbo, *Phys. Rev. Lett.*, **10** (1963)531; M. Kobayshi And T. Maskawa, *Prog. Theor. Phys.*, **49** (1973) 652.
- [35] L. Wolfenstein, *Phys. Rev. Lett.* **51** (1983) 1945.
- [36] S. Stone, *Prospects for B-Physics in the Next Decade*, Presented at NATO Advanced Study Institute on Techniques and Concepts of High-energy Physics, St. Croix, U.S. Virgin Islands, July 1996, in *St. Croix 1996, Techniques and concepts of high-energy physics IX* p465, hep-ph/9610305.

- [37] Y. Kubota et al. (CLEO), *Nucl. Instr. and Meth. A* **320** (1992) 66. H. Albrecht et al. (ARGUS), *Nucl. Instr. and Meth. A* **275** (1989) 1.
- [38] I. Caprini and M. Neubert, *Phys. Lett. B* **380** (1996) 376; M. Shifman et al., *Phys. Rev. D* **51** (1995) 2217; Erratum-ibid. D52 (1995) 3149; A. Czarnecki, *Phys. Rev. Lett.* **76** (1996) 4124; T. Mannel, *Phys. Rev. D* **50** (1994) 428; A. F. Falk and M. Neubert, *Phys. Rev. D* **47** (1993) 2965 and 2982.
- [39] M. Margoni et al., (DELPHI), *Measurement of V_{cb} Using the Identified Charged Pion in $\bar{B}^0 \rightarrow D^{*+}\ell^{-}\bar{\nu}$* , DELPHI 98-140, (1998).
- [40] D. Buskulic et al. (ALEPH), *Phys. Lett. B* **395** (1997) 373.
- [41] K. Ackerstaff et al. (OPAL), *Phys. Lett. B* **395** (1997) 128.
- [42] B. Barish et al. (CLEO), *Phys. Rev. D* **51** (1995) 1014. The CLEO value has been boosted by 2.6% to account for the expected negative curvature near $\omega = 1$, see S. Stone, *Probing the CKM Matrix with b Decays* in Proc. of *The Albuquerque Meeting*, ed. S. Seidel, World Scientific, Singapore (1994) 871.
- [43] R. Fulton et al. (CLEO), *Phys. Rev. Lett.* **16** (1990) 64; H. Albrecht et al. (ARGUS), *Phys. Lett. B* **234** (1990) 409.
- [44] M. Battaglia et al. (DELPHI), *Measurement of $|V_{ub}|/|V_{cb}|$ with DELPHI at LEP*, DELPHI 98-97 CONF 165 submitted to the XXIX Int. Conf. on High Energy Physics, Vancouver, #241 (1998).
- [45] N. G. Uraltsev, *Int. J. Mod. Phys. A* **11** (1996) 515; I. Bigi et al., *Annu. Rev. Nucl. Part. Sci.*, **47** (1997) 591.
- [46] C. Jin, *Extracting $|V_{ub}|$ from the Inclusive Charmless Semileptonic Branching Ratio of b Hadrons*, hep-ph/9810427 (1998).
- [47] N. Isgur and D. Scora (ISGW II), *Phys. Rev. D* **52**, (1995) 2783; N. Isgur, D. Scora, B. Grinstein, and M. B. Wise, *Phys. Rev. D* **39**, 799 (1989); M. Wirbel, B. Stech and M. Bauer *Z. Phys. C*29, 637 (1985); M. Bauer and M. Wirbel (WBS), *Z. Phys. C* **42** (1989) 671; J. G. Korner and G. A. Schuler (KS), *Z. Phys. C* **38** (1988) 511; ibid, (erratum) *C* **41** (1989) 690; D. Melikhov, *Phys. Rev. D* **53** (1996) 2460; G. Altarelli et al.(ACM), *Nucl. Phys. B* **208** (1982) 365; C. Ramirez, J. F. Donoghue and G. Burdman (RDB), *Phys. Rev. D* **41** (1990) 1496.
- [48] R. Barate et al. (ALEPH), *Determination of $|V_{ub}|$ from the Measurement of the Inclusive Charmless Semileptonic Branching Ratio of b hadrons*, (CERN-EP-98-067) 1998 submitted to *Eur. Phys. Jour. C*.
- [49] M. Acciarri et al. (L3), *Phys. Lett.*, B **436** (1998) 174.
- [50] J. Bartelt et al. (CLEO), *Phys. Rev. Lett.* **71** (1993) 4111.
- [51] J. P. Alexander et al. (CLEO), *Phys. Rev. Lett.* **77** (1996) 5000.
- [52] B. Eržen et al. (DELPHI), *Measurement of $|V_{cs}|$ using W decays at LEP2*, DELPHI-98-107 (1998).